

# Some topological features of the entrainment process in a heated turbulent wake

By J. A. FERRÉ AND FRANCESC GIRALT

Departament d'Enginyeria Química i Bioquímica, Divisió VII, Universitat de Barcelona,  
43005 Tarragona, Catalunya, Spain

(Received 2 October 1987 and in revised form 9 May 1988)

The temperature signals measured in a fully turbulent, thermally contaminated wake behind a heated cylinder at  $x/D = 140$ , are analysed using a pattern-recognition procedure. The temperature patterns detected show that the wake flow is dominated by shear-aligned structures with a strong three-dimensional character. The temperature footprints have a limited extent in the spanwise and streamwise directions, while their dimension is of the order of the wake width in the vertical coordinate. The footprints are characterized by a steep temperature gradient at their back edge, which appears as a sharp hot-to-cold transition. The topological features inferred from the temperature signals suggest that the entrainment process is accomplished mainly by engulfing external fluid. The large-scale organized structures are interpreted as the temperature footprints of the double-rollers characterizing the large-eddy motion in far wakes. The analysis of present results within the context of previous studies about intermittency in heated wakes, brings forward the idea that the intermittent bulges are the emerging double rollers at the three-dimensional turbulent/non-turbulent interface.

---

## 1. Introduction

In a previous paper, Ferré & Giralt (1989, hereinafter referred as FG), developed a pattern-recognition technique for the analysis of large-scale motions in turbulent flows. The technique was applied to examine the large-eddy organization of several wakes with different initial conditions. Here, this previous velocity analysis is extended to the temperature signals measured in the turbulent wake generated by a heated cylinder, at  $x/D = 140$  and  $Re = 9000$ . The main objective is to identify the temperature footprints of the large-scale motions, such as double-roller eddies, previously detected and identified in fully developed turbulent wakes by Mumford (1983) and FG.

Several authors have used thermally contaminated wakes in the past to study the details of the entrainment process and to determine the statistics of the turbulent/non-turbulent interface. LaRue & Libby (1974*a*) examined the wake behind a single heated cylinder at  $x/D = 400$ , by means of auto and cross-spectral analysis of the temperature and intermittency signals. They observed that interface bulges were related to the large-scale structure of the bulk flow, a result that was consistent with the large eddies proposed by Grant (1958). Moreover, these authors found that the transverse axis of the structures were inclined at an average angle of  $31^\circ$  with respect to the vertical axis, providing evidence of shear alignment in the temperature field of the wake.

LaRue & Libby (1974*b*) obtained in a subsequent publication ensemble averages

of the temperature footprints of the intermittent bulges. Results showed that the central parts of the bulges were occupied by well-mixed fluid (old turbulence) followed by a relatively high temperature gradient at the back edges of the bulges. Furthermore, since the front interfaces of the intermittence bulges were observed to present a lower temperature gradient, LaRue & Libby (1974*b*) suggested that most entrainment occurred at these front edges.

One of the few works related to the determination of the spanwise structure of a plane turbulent wake is that of Barsoum, Kawall & Keffer (1978). They analysed the space-time correlation of the intermittence function at  $x/D = 100$  and concluded that the interface bulges were strongly three-dimensional and non-periodic. The extent of these bulges in the spanwise direction was less than in the streamwise direction, but greater than in the lateral direction.

Kawall & Keffer (1982) examined the development of a uniformly strained turbulent wake behind a heated cylinder. Results indicated that even when the mean velocity and temperature profiles were self-similar, the scales derived from the r.m.s. profiles and from the mean position of the intermittent bulges changed during distortion at a rate significantly different from that required for self-preservation. This lack of self-preservation was attributed to the amplification of the action of coherent structures by the distorting field. The presence of coherent structures was detected by spectral analysis of the  $u$ - and  $v$ -velocities and, in particular, by the one-point coherence function of the  $w$ -signal. The contribution to the coherence function was mainly from the quad-spectrum, while the cospectrum (and then the cross-correlation) was nearly zero.

Fabris (1979) performed a detailed conditional sampling analysis of the plane wake at  $x/D = 400$ , using a special-purpose four-wire probe. He measured simultaneously the three components of the velocity vector and temperature. In a subsequent paper, Fabris (1984) reported results concerning the conditional analysis of the interaction of two wakes, with one of them thermally contaminated. One of the most interesting results reported in the first publication is that the patches of potential flow were moving faster ( $u$ -velocity) than the mean flow, while the contrary was observed for the turbulent bulges. In addition, conditional  $v$ -velocity measurements showed that while the potential flow moved towards the centre of the wake, the turbulent flow moved away from the wake. Also, the conventional averaged  $v$ -velocity had a small negative value corresponding to a net inflow towards the centre of the wake.

A more recent paper by Browne, Antonia & Bisset (1986) deals with characterization of coherent structures in the far field of a turbulent wake. Although the results presented in this work correspond to the velocity field in the vertical plane of the wake, the detection scheme used was based on a conditional sampling procedure triggered by temperature gradients simultaneously sensed by an array of thermometers equally spaced in the spanwise direction. These results can provide further evidence of the link between the structures observed in the velocity field of the far wake (Mumford 1983; FG) and those presented here, and will be referred to in some detail in §5.

The aim of the present work is to apply the pattern-recognition approach in order to study the temperature signals sampled by a set of six thermometers in the far wake ( $x/D = 140$ ) of a cylinder, so that the temperature footprints of the double-roller eddies and the  $\omega_z$ -vortices, identified in previous studies (Mumford 1983; FG), can be analysed. Once the relation between these structures and the temperature footprints is established, the mechanism of entraining external, cold, fluid by engulfing will be examined. In the following sections a description of the experimental

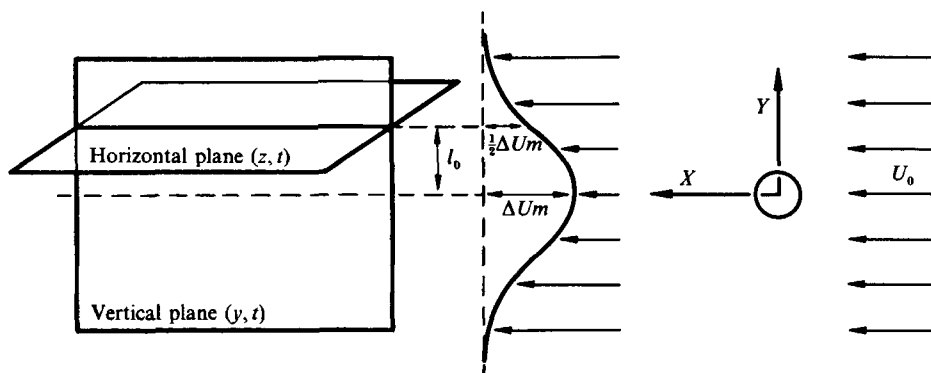


FIGURE 1. Flow configuration and planes of measurement.

arrangement used, some specific details of the pattern-recognition analysis applied to the temperature signals, the organized structures detected in the thermal field and their relation with those of the velocity field and the discussion about entrainment are presented.

## 2. Experimental equipment and data acquisition

The wake investigated was generated in an open-circuit, suction-type wind tunnel, with an experimental section 60 cm square and 3 m long. A set of flow straighteners, filters, and a 9:1 contraction zone produced a low-turbulence (less than 0.4%) free-stream flow, that could be continuously controlled from 2 to 20 m/s by means of a variable speed fan. The wake was generated by placing a cylinder with a diameter of 12 mm normal to a free stream of 11.3 m/s, which yielded a Reynolds number of 9000. Heat was supplied by an electrical resistance of 65 ohms, placed inside the cylinder and operated at 200 V. This produced a mean temperature difference between the wake and potential flow of 1 °K at  $x/D = 140$ , with maximum temperatures approximately 2 °K above the potential value. Measured mean and r.m.s. temperature profiles and scales were in good agreement with those reported by Beguier, Giralt & Keffer (1978) for similar experimental conditions.

The data acquisition system was a 12-bit A/D converter linked to a PDP 11/60 computer. The voltage signals were offset to zero, amplified, low-pass filtered at 2 kHz and sampled at 5 kHz per channel over 50 s. The low-pass filters were second-order IIR Butterworth filters. Once digitized, the voltage signals were copied onto magnetic tapes and processed in an IBM 3083 computer at CIUB (Informatic Centre of the University of Barcelona).

Six constant-current thermometers (DISA 55M01/55M20 bridges and 55P31 probes) operated at 100 mV/°K, approximately, were used to measure the instantaneous temperatures in the wake studied. The thermometers were calibrated in the empty working section of the wind tunnel, with temperatures determined to 0.01 °C with a reference thermometer. Data acquisition was performed separately in two perpendicular planes as shown in figure 1. The spacing between anemometers was selected to be  $0.6l_0$ , so that the whole region of flow with significant velocity defect in the vertical plane ( $y, t$ ), as well as an equivalent region in the horizontal plane ( $x, t$ ), were covered. Note that the half width of the wake defined from the mean velocity profile is  $l_0 = 3.3D$  at  $x/D = 140$ .

### 3. Pattern-recognition analysis of the temperature signals

The pattern-recognition technique used has been described elsewhere (FG). Thus, only the relevant aspects pertaining to the analysis of the temperature signals will be presented here.

Most of the previous experimental studies performed in heated flows have been carried out by obtaining from the temperature signals an intermittency function to discriminate the turbulent (hot) and non-turbulent (cold) bulges within the flow. The introduction of a set of thermometers simultaneously sensing temperatures in the wake, initially suggested the possibility of obtaining instantaneous intermittency maps. While the 5 kHz sampling rate gave sufficient temporal resolution for this purpose, the spatial resolution in the transverse direction, which is determined by probe spacing, was about an order of magnitude worse and almost certainly inadequate.

$U$ -velocity and temperature signals sampled at  $x/D = 140$  in the cold wake of a single cylinder and in the wake of the heated cylinder are shown in figures 2(a) and 2(b), respectively. This figure clearly illustrates the intrinsic differences between the velocity and temperature signals, and why it is so easy to derive the intermittence function from temperature measurements (figure 2b). The effect of the turbulent/non-turbulent interface crossing the set of anemometers is also noticeable but not so evident in the  $u$ -velocity field depicted in figure 2(a).

It should be noted that in the previous analysis of the velocity field (FG) it was possible to deduce the structural organization of the flow without taking intermittency into account. These facts supported the analysis of the temperature signals with the same pattern-recognition method used in FG for the velocity signals and, thus, excluding the instantaneous intermittency maps as a convenient analytical procedure. As a consequence all temperatures measured in the wake were normalized subtracting their mean values and dividing by their r.m.s. values. When the thermometers were placed in the  $(z, t)$  horizontal plane the r.m.s. values used to normalize the data were those measured at each individual position, while for measurements in the vertical plane a pooled estimate of the r.m.s. was used.

For velocity signals, subtraction of the time-mean velocity implies, implicitly, assuming some hypothesis on the convection velocity of organized structures. In the case of the temperature signals, this procedure discriminates 'colder' from 'hotter' patches in the temperature records, instead of cold (temperature equal to that of the potential flow temperature) from hot (temperature just above the cold one) patches. Obviously cold and hot are synonymous to potential and turbulent flow, but 'colder' and 'hotter' can be loosely interpreted as 'younger', or recently entrained fluid, and 'older' fluid, which has been turbulent for some time, respectively. Despite the arbitrariness of subtracting the time-mean temperature, there was no reason to suppose that any other temperature would have been a more reasonable choice. For this reason, all results presented have to be interpreted assuming that the 'hotter' zones correspond to true turbulent motions, and the 'colder' ones, while not necessarily corresponding to the passage of potential flow, should be related to the fluid that is younger than the mean flow in the wake. Thus the latter represent the pockets of irrotational fluid that are being entrained or that, having been entrained upstream, are still not well mixed with the turbulent flow and retain part of their 'potential' identity.

The plots of organized structures will be presented as iso-level contours of the ensemble-averaged temperature fluctuations, at  $\pm 10\%$ ,  $\pm 25\%$ ,  $\pm 50\%$  and  $\pm 75\%$

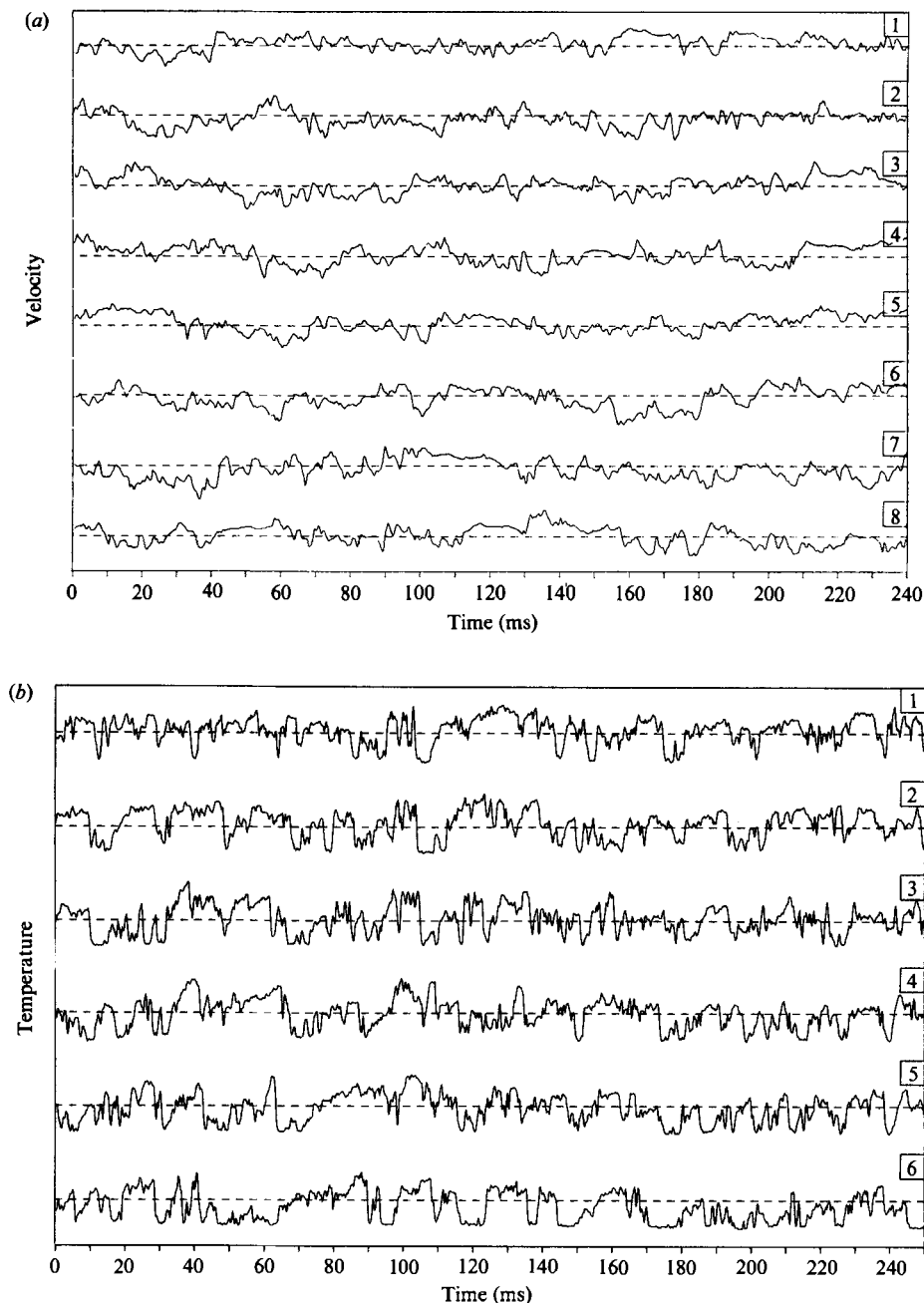


FIGURE 2. Turbulent signals at  $x/D = 140$ . (a)  $u$ -Velocities. (b) Temperatures.

of the peak temperature signal. Arrowheads have been added at positions where sensors are placed to show the sign and magnitude of the averaged quantities. The horizontal axis is the time coordinate, increasing towards the right, and the vertical axis is the spatial coordinate ( $z$  or  $y$ ). Arrowheads are scaled to show the magnitude of the ensemble-averaged temperatures with respect to the mean values, and are directed towards the left for negative values and towards the right for positive ones.

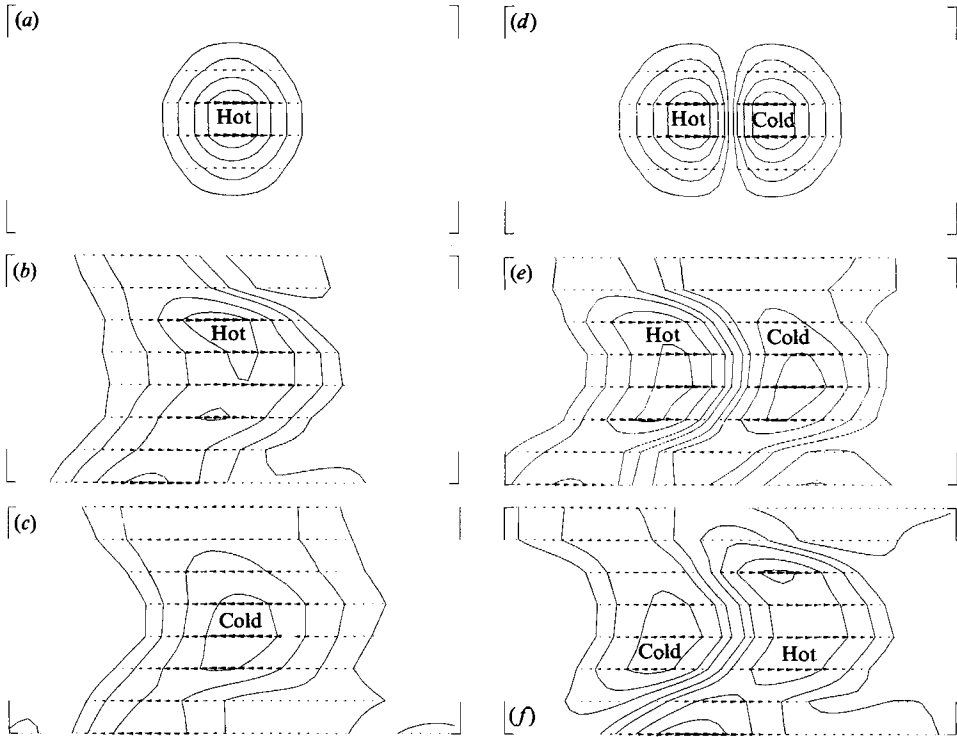


FIGURE 3. Temperature patterns in the vertical plane. (a) Single prototype. (b) Hot temperature strips. (c) Cold temperature strips. (d) Hot and cold prototype. (e) Hot-to-cold temperature strips. (f) Cold-to-hot temperature strips.

Both axes have the same scaling, thus the patterns presented are in ‘natural’ coordinates (time units are converted into space units using the free-stream velocity  $U_0$ ). Since the probe spacing is  $0.6l_0$ , all the ensemble averages presented will be  $0.6(N-1)l_0$  high and  $1.2(N-1)l_0$  wide for  $N$  anemometers in the ensemble-averaging window. In the present analysis a value of  $N = 8$  for the test pattern was used to allow the effective search of all, aligned and misaligned, structures convected over the six sensors.

Initial temperature patterns or templates have been generated by a Gaussianly damped stream function,

$$\psi(x, y, z) = \psi_0 f\left(\frac{x}{x_0}, \frac{y}{y_0}, \frac{z}{z_0}\right) \exp\left\{-\frac{1}{2}\left[\left(\frac{x}{x_0}\right)^2 + \left(\frac{y}{y_0}\right)^2 + \left(\frac{z}{z_0}\right)^2\right]\right\}, \quad (1)$$

so that cold and hot temperature spots can be easily simulated as negative or positive stream-function values, with intensity and spatial extent controlled by the  $\psi_0$ ,  $x_0$ ,  $y_0$  and  $z_0$  scaling parameters. When  $f(x/x_0, y/y_0, z/z_0) = x/x_0$ , for example, (1) yields the template shown in figure 3(d).

The fraction of flow represented by an ensemble, the peak temperature signal and the level of significance of the lowest isocontours associated to each ensemble average, constitute a measure of how significant the results obtained with the pattern recognition code are (FG). The level of significance† depends not only on the peak

† The level of significance is defined as the probability of recognizing by chance a non-identity as a pattern. A zero level thus means absolute certainty.

signal but also on the number of patterns detected, because higher levels can be achieved by scanning more data, regardless of how low the detection frequencies are. This is the reason why both measures, the fraction of flow represented by one ensemble average and the level of significance, have to be presented in order to assess the importance of the organized motions detected.

#### 4. Structural characteristics of the thermal field

##### 4.1. Footprints sensed in the vertical plane

The analysis of the velocity signals in the vertical plane of the wake behind a single cylinder (FG), showed that at  $x/D = 140$  any kind of  $\omega_z$ -vortices appeared contaminated or dominated by shear alignment. As a consequence, our first analysis in the vertical plane of the heated wake was directed to further investigate this aspect. The initial template used was again a guess for what we believed could be the temperature footprints of vortices with  $\omega_z$ . This is presented in figure 3(a). The ensemble average obtained after three iterations of the pattern recognition program is shown in figure 3(b). The peak velocity signal is 1.36 and the significance level is low (0.10%), but only 25% of the recorded flow contributed to the average.

There are three aspects of figure 3(b) that are worth commenting on. First, the ensemble-averaged temperature structure spans the full width of the wake, despite the limited extent of the closed contours in the initial pattern, showing that the anemometers are sensing temperature strips instead of bulges of finite extent in the vertical direction. Secondly, these temperature strips display a clear shear alignment (time increases towards the right, so the flow is moving from right to left) despite the symmetry of the initial pattern. The angle of alignment is consistent with the  $31^\circ$  reported by LaRue & Libby (1974a). Finally, the small zone with negative temperature (colder fluid) that appears at the top right of the ensemble, also maintains the general shear alignment shown by the whole organized structure.

In the heated wake only the hotter spots can be assumed to be fully turbulent, so that no organized activity is expected to be associated to the colder bulges. However, the appearance of the small aforementioned cold region in figure 3(b) induced the repetition of the previous analysis but searching for cold structures instead of hot ones. The ensemble average so obtained is presented in figure 3(c), where the relevant parameters are very similar to those of figure 3(b). Surprisingly, the colder flow in the wake shows an organization that is a copy of that detected for the hotter patches. A possible explanation of that fact is that the colder flow simply fills the void spaces between consecutive hot organizations. If this were the case, an initial pattern containing a hot + cold arrangement, like that presented in figure 3(d), would capture the flow organization containing simultaneously both the hot and cold strips observed before.

The ensemble averages obtained from the prototype of figure 3(d), when selecting positive or negative-correlated data frames, are those presented in figures 3(e) and 3(f). Their peak temperature values are 0.83 and 0.92, respectively, and the level of significance is less than 0.5% in both ensembles. The peak temperature signals obtained are lower than those corresponding to the previous ensemble averages included in figures 3(b) or 3(c). However, the fraction of flow classified when searching for the patterns in both figures 3(e) and 3(f) is over 50%, approximately doubling the fraction obtained when classifying the wake as independent hot or cold strips (figures 3(b) or 3(c)).

It is interesting to analyse in detail the whole set of results presented in figure 3,

together with the peak velocity values obtained and the fraction of flow classified in each case. It is clear that when combined hot + cold temperature strips are selected, rather than hot or cold patches, the fraction of flow doubles. The cause is that the data windows contributing to figures 3(b) and 3(c) are exclusive, while both kinds of data frames are accepted in the ensemble averages of figures 3(e) and 3(f). However, it remains to explain why the pairing hot + cold (or cold + hot) appears only very weakly in figure 3(b). The answer could be that this pairing does not have a constant spacing, so that when the initial prototype does not explicitly contain a temperature gradient, the ensemble average smears out the surrounding information. This also explains the lower peak signal value of figures 3(e) and 3(f). As a consequence of the temperature gradient that forces the alignment, the maximum and minimum temperature values reach lower values than in figures 3(b) and 3(c).

The similarity between the individual hot and cold temperature strips depicted in figures 3(b) and 3(c), or those of figures 3(e) and 3(f), together with the impossibility of selecting the dominating organization among the two of figures 3(e) and 3(f), lead to the conclusion that the typical organization of the flow sensed when measuring in the vertical plane should be a succession of hot + cold + hot + ... + cold strips without a preferred spacing, in accordance with the random character of the temperature field observed by LaRue & Libby (1974*a*) and Barsoum *et al.* (1978), among others.

LaRue & Libby (1974*a*) obtained evidence not only of a symmetrical structure in the wake, but also of an antisymmetrical organization. A re-examination of the data in the  $(y, t)$ -plane, using an initial pattern such as that of figure 4(a), explicitly containing hot and cold flow at the same vertical position, was thus necessary. The ensemble average obtained after three iterations, shown in figure 4(b), has a peak temperature signal of 1.1 r.m.s. units and the fraction of flow represented by the ensemble is 59% with a significance level less than 0.01%.

Note that the results in figure 4(b), while displaying antisymmetrical features do not contradict the more clear symmetrical arrangements of figures 3(e) and 3(f). Furthermore, it has to be realized that the individual patterns contributing to the ensemble averages in these figures are not mutually exclusive because transverse alignment was allowed during the search. This explains why the fraction of flow represented by the patterns in figures 3(e) or 3(f) and 4(b) account for more than 100%. Shear alignment again dominates the pattern in figure 4(b). In this case several hot-to-cold transitions develop after iteration without being present in the initial pattern.

Wynanski, Champagne & Marasli (1986) showed that the far wake is subject to instability with both symmetrical and antisymmetrical modes. On the basis of present results in figures 3 and 4 it is difficult to decide which of the symmetrical or antisymmetrical organization is dominant, because an antisymmetrical structure displaced from the wake centre plane can be interpreted as a symmetrical one, and vice versa. The most important difference between both types of patterns is that the antisymmetrical one seems more appropriate to educe temperature gradients, even when these have not been included in the template, particularly hot-to-cold transitions, which will be shown later to be a characteristic also appearing in the horizontal plane. Otherwise, the plots of figures 3 and 4 are not only consistent with the observation that lumps of cold fluid can be occasionally detected at the centre of the wake, but also show that deep penetrations of 'colder' fluid towards the centre



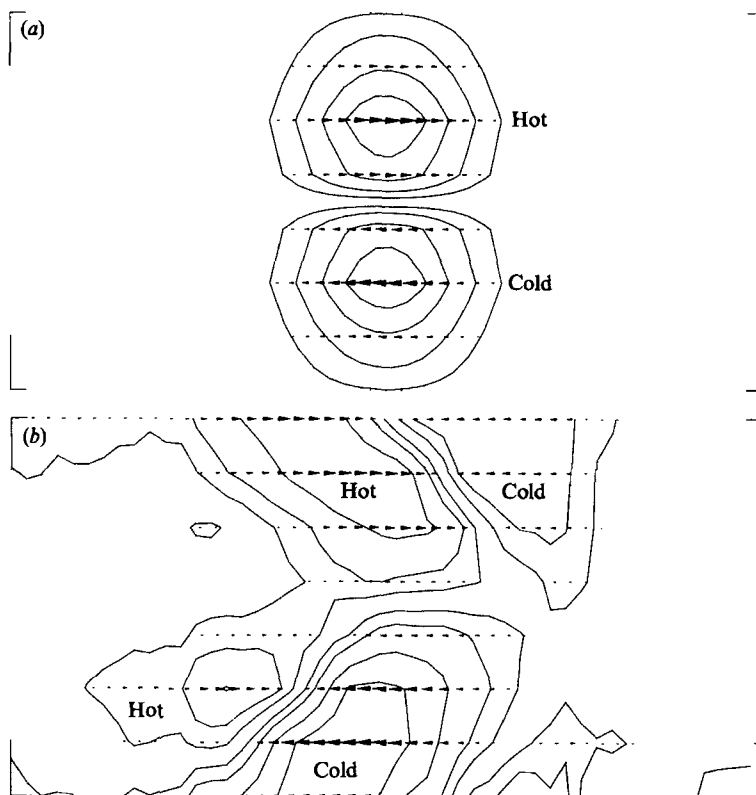


FIGURE 4. Antisymmetric thermal structures. (a) Prototype. (b) Ensemble average after three iterations.

occur in an ordered manner, maintaining a typical organization for distances of the order of the wake width.

Present results clearly indicate that alignment with the mean rate of strain dominates the temperature field of the wake when observed in a vertical slice. To explain this alignment it has to be understood that only the large-scale ordered motions with a high content of vorticity can prefer such orientation in order to take advantage of vortex stretching to extract energy from the mean flow. Therefore, the temperature patterns depicted in figures 3 and 4 and which are so clearly aligned, have to be related to the shear aligned double-roller eddies observed by Mumford (1983) and FG. Nevertheless, while this leads to acceptance of the idea that the hotter aligned strips are the temperature footprints of the rollers, it remains to be explained why the colder ones, with a smaller vortical content†, do not appear with a more random orientation. It seems to us that a reasonable explanation is that the hot large-scale ordered structures observed in the wake organize the penetration of the colder fluid and, thus, are responsible for the entrainment process by engulfing.

The omnipresent alignment of the large scales with the direction of positive rate of strain in the vertical plane of measurement and their striped shape with open isotherms suggest that the  $\omega_z$ -vortices reported by Townsend (1979) cannot exist as

† Thermal and vortical contamination of external flow should take place at similar rates since  $Pr \approx 1$  in air.

independent and isolated spanwise structures, but perhaps only as the outer parts of the shear-dominated organization of the wake. Furthermore, the results in the horizontal plane presented in the following section show that the wake is strongly three-dimensional and that any  $\omega_z$ -structure should have a very limited spanwise extent. A similar but not so definitive conclusion was drawn from the analysis of the velocity signals in the far wake (FG). In this sense, the velocity patterns that should be associated to the temperature footprints of figure 3 are those observed by Mumford in the vertical centre plane of the wake (Mumford 1983).

As discussed before, only the hotter patches can be unambiguously identified as turbulent flow, while the colder ones should be a mixture of recently entrained and truly cold fluid. If a temperature lower than the time-mean value was subtracted from the signals, the cold patches would reduce in size and it would be progressively more difficult to identify the deep penetrations of colder fluid towards the centre of the wake. This is the reason why an analysis based upon intermittency maps would never succeed in identifying such flow organization. This fact is also related to the conditional p.d.f. measurements of Thomas (1973). He observed a strong non-Gaussian character in the conditional p.d.f. of the turbulent  $u$ -velocities, while the irrotational ones behaved approximately normally. He suggested that this departure from normality could have been produced by the influence of the newly entrained fluid that, despite being classified as turbulent, retained a higher  $u$ -velocity content. The two conditional p.d.f. measured by Thomas peaked very closely, the turbulent one showing a long tail of low  $u$ -velocities. A similar effect, after changing defect by excess velocities, was observed by Mumford (1973) in a plane jet, though in the latter case the two p.d.f. peaked more separately.

In view of the structural characteristics of the thermal field in the far wake, the results reported by Thomas (1973) can be interpreted as the gradual conversion of the engulfed pockets of irrotational flow into turbulent flow. During the first stages of mixing, the irrotational pockets are progressively contaminated by heat and vorticity. Simultaneously they deliver progressively momentum to the bulk turbulent flow. Since any intermittency-detection scheme does not assign 'ages' to non-potential pockets, some of them, regardless of being classified as turbulent, still retain a 'free-stream' identity, associated with a higher  $u$ -velocity content. This explains the form of the conditional p.d.f. measured by Thomas (1973).

Finally, it remains to examine the performance of the pattern-recognition technique. While the initial prototypes of figures 3(a) and 3(d) are formed by closed isotherms, the pattern-recognition procedure identifies without difficulty the striped organization of the thermal field. Furthermore, irrespective of the orthogonality between the prototypes of figures 3(d) and 4(a) in the pattern space (FG), the technique is able to converge in both cases to ensemble averages that display the same kind of organization of the flow. In both cases the results have been obtained after three iterations. These results show that the pattern-recognition approach developed can be used in situations where a previous knowledge of the characteristics of the flow is limited or even erroneous.

#### 4.2. *Footprints sensed in the horizontal plane*

The analysis of the velocity signals sensed with anemometers located in the  $(z, t)$ -plane of the wake, provided evidence that the typical large-scale structures were double-roller eddies. Single rollers had to be considered as double rollers partially sensed by the array of anemometers (FG). However, temperature signals cannot distinguish single from double rollers if both are turbulent (hot) flow structures.

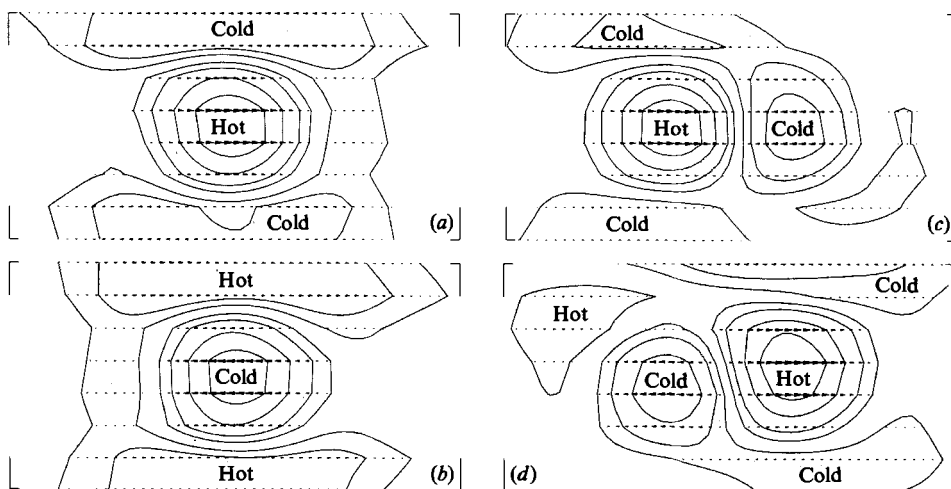


FIGURE 5. Temperature patterns in the horizontal plane. (a) Hot temperature spots. (b) Cold temperature spots. (c) Hot temperature spots and hot-to-cold gradients. (d) Hot temperature spots and cold-to-hot gradients.

Thus, the prototype for the double-roller recognition in the thermal field was the temperature pattern already used in the  $(y, t)$ -plane and which is presented in figure 3(a). When this pattern was used as initial template, the averages obtained were those shown in figure 5(a), for positive correlated data frames, and in figure 5(b), for negative correlated temperature fluctuations (a situation that corresponds to a search for cold spots). The fraction of flow classified is 51% and 48%, respectively. For both ensembles the peak temperature value is 1.1 r.m.s. units and the level of significance is lower than 0.05%.

A common characteristic of both ensemble averages presented in figures 5(a) and 5(b) is not only that the patterns with closed isotherms are maintained, but additional sign-inverted temperature lobes appear bounding the hot or cold spots in the spanwise coordinate. Remembering the results obtained in the vertical plane, one cannot attribute this feature to the form of the initial pattern but should recognize the strong three-dimensional character of the flow structures, which have a very limited extent in the spanwise direction. Perhaps the most striking feature of figures 5(a) and 5(b) is that the sign-inverted temperature lobes that appear in the spanwise direction join each other, enclosing the central temperature spot in the streamwise direction. This provides evidence of temperature gradients corresponding to hot-to-cold transitions, again from an initial prototype that was unbiased in favouring this feature or its opposite (cold-to-hot transitions).

As in the vertical plane, this last observation suggested that an initial pattern containing a sharp temperature change, such as that depicted in figure 3(d), could extract this feature more efficiently. The ensemble averages obtained for hot-to-cold and cold-to-hot transitions are shown in figures 5(c) and 5(d), respectively. The fractions of flow averaged are 63% and 59% and the peak temperatures 0.96 and 0.92, respectively. The significance levels are well below 0.1%. One can observe that the symmetry previously displayed by figures 5(a) and 5(b) is lost in figures 5(c) and 5(d), which show a predominant hot bulge surrounded almost everywhere by cold flow. Both cold-to-hot and hot-to-cold temperature gradients also appear in these

figures in the front and back edges of the hot spot. However, only the hot-to-cold gradient in the back edge is sharp enough to develop in both figures 5(a) and 5(b) from an initial template that has no change of sign, like that in figure 3(a).

When only figures 5(a) and 5(b) are analysed, their similarities suggest that the actual temperature patterns sensed in the horizontal plane could be a patched distribution of hot and cold spots. However, figures 5(c) and 5(d) strongly suggest that the typical organization at the half width of the wake, which approximately coincides with the maximum shear stress position, tends to be a hot spot surrounded by cold fluid. Moreover, the strip character of the temperature patterns sensed in the vertical plane (figures 3 and 4), puts forward the idea that this could also be the typical organization for a wide range of  $y$ -locations, perhaps from  $y = 0$  to  $y \approx \pm 2l_0$ .

The genuine feature in the horizontal plane is the strong three-dimensional character of the temperature structures which could not be deduced, or even suspected, from the results in the vertical plane. In view of these results it is difficult to argue that 'pure' spanwise vortices could exist in the far wake as their  $z$ -extent should be smaller than  $2l_0$  units, approximately. Taking into account that the patterns obtained are only colder and hotter temperature spots and not true intermittence signals, present results agree pretty well with the typical temperature footprints of the intermittent bulges observed by LaRue & Libby (1974b), particularly with respect to the sharp back edges of the turbulent bulges that generate such a steep hot-to-cold temperature gradient.

## 5. Final discussion

The typical organization of the temperature field in the vertical plane of the wake is an open-isotherm ensemble average (see figure 3), with no special thermal organization linked to  $\omega_z$ -vortices. This finding is further supported by the limited extent of the temperature structures in the spanwise direction when observed in an horizontal plane. This lack of identity leads us to suggest that the  $\omega_z$ -vortices reported by Townsend (1979) should be part of the dominant shear-aligned organization extending the vertical plane of the wake (see figure 3). The problem arises when one tries to relate the temperature patterns so far presented, the double rollers observed by Mumford (1983) in the far wake and by FG in a family of wakes and the  $\omega_z$ -vortices of Townsend. Unfortunately, simultaneous measurements of temperatures and velocities in the far wake are not yet available and a point-by-point equivalence between these flow organizations cannot be established at present. However, there are some features of the observed structures that strongly support the hypothesis that the temperature patterns observed are the thermal footprints of the double rollers that dominate flow in the far wake.

First, it has to be noted that the temperature strips in the  $(y, t)$ -plane are consistent with the velocity footprints detected by Mumford (1983) in the vertical plane of the wake. He observed that some double rollers extended over the centre wake, while some others were located on one side only. This situation corresponds to the temperature patterns of figures 3 and 4, respectively. Secondly, it is clear that the hot spots are extremely sensitive to alignment with the mean rate of strain, which not only confirms their vortical (and then turbulent and coherent) character, but suggests that the mechanism of vortex stretching dominates the configuration and dynamics of the large-scale structures in plane turbulent wakes. Moreover, the temperature patterns in the horizontal plane of the wake retain the three-dimensional

character that one hoped to observe if the double rollers were the true organization of turbulence and the flow not contained in these eddies were the irrotational (colder) flow filling the 'voids' in the wake.

An independent indication that the temperature patterns are related to vortex stretching in the wake, is provided when present results are compared with those of Browne *et al.* (1986). They used a conditional sampling procedure triggered by spanwise temperature gradients (hot-to-cold transitions) simultaneously sensed by an array of sensors spanning  $0.8l_0$ . It can be easily checked in figure 5, where the spacing between measuring points is  $0.6l_0$ , that this is effectively a little less than the spanwise extent over which the temperature gradient maintains its identity. Moreover, the conditional measurements reported by Browne *et al.* (1986) were carried out with a  $\times$ -wire centred with respect to the array of thermometers. Therefore, their conditional averages should be interpreted as the vertical and centred slice of the double rollers, as long as these are associated to the temperature gradients, rather than being considered the large-scale 'spanwise' structure of the wake, because the results in figure 5 show that temperature gradients in a horizontal plane not only have a very limited extent, but are effectively bounded by colder fluid. Anyway, they observed that these temperature fronts coincided with the zones of vortex stretching in the dynamic field of the far wake.

The general feature of the temperature gradients detected by Browne *et al.* (1986) is an antisymmetrical structure with alternate temperature fronts at each side of the wake, in accordance to the temperature organization shown in figure 4. However, a detailed examination of the detection procedure used in that publication reveals that this is just one of the possible configurations. Thus, the coexistence of double-roller structures, some of them spanning the full width of the wake, some confined to just one side, has to be accepted as a feature of the wake flow and not merely as a consequence of the failure to observe some preferred mode.

During the discussion of the results presented in the previous sections, it was considered that the hotter structures were responsible for the entrainment process by engulfing. After having hypothesized that the thermal structures observed are the temperature footprints of the double rollers, it is appropriate to re-examine this possibility in view of the results reported by LaRue & Libby (1974*a, b*) and Fabris (1979). LaRue & Libby reported that the intermittent bulges were well correlated with the temperature structures of the inner wake. From the present set of observations, it seems that the intermittent bulges are the double rollers emerging towards the edges of the wake which organize the entrainment process, determine the growth of the wake and, indirectly, control the transfer of energy from the mean flow. This is supported by the findings of Fabris (1979), who observed that the old, turbulent flow, moved towards the edges of the wake while the cold potential flow moved into the wake, the global balance being a weak, though measurable, negative  $v$ -velocity responsible for net inflow (entrainment) into the wake.

The entraining mechanism has to be linked to the differences observed between the front and back edges of the hot spots or bulges. A way to reconcile the fact that entrainment seems to be controlled by the double rollers and to occur mainly at the front edges of the bulges, as suggested by LaRue & Libby (1974*b*), is to assume that the double rollers have a preferred sense of rotation, characterized by backflow in its centre, and that they are connected at their external edge, forming a horseshoe-like vortex line. If this was the case, the top of the rollers (which should have spanwise vorticity), as well as their legs (with shear aligned vorticity) should be both

responsible for entrainment by engulfing and subsequent mixing of external cold fluid, a situation that is consistent with present and previous experimental evidence of a more thoroughly mixed region at the front edges of the bulges.

Moreover, if the double-roller eddies are responsible for the entrainment process, they might control the input of energy from the potential flow that is fed to the energy cascade in the wake. In addition, if the double rollers are associated to vortex stretching, they have to be also the parts of the flow where high production and dissipation occur and, in general, the regions of the wake where the activity of the fine scales concentrates. These aspects are currently being investigated.

Financial assistance received from the CICYT, the CIRIT and the Servei de Tecnologia Química is acknowledged.

#### REFERENCES

- BARSOUM, M. L., KAWALL, J. G. & KEFFER, J. F. 1978 *Phys. Fluids* **21**, 157–161.
- BEGUIER, C., GIRALT, F. & KEFFER, J. F. 1978 *Proc. Intl Heat Trans. Conf. Toronto*, vol 5, pp. 353–358.
- BROWNE, L. W. B., ANTONIA, A. A. & BISSET, D. K. 1986 *Phys. Fluids* **29**, 3612–3617.
- FABRIS, G. 1979 *J. Fluid Mech.* **94**, 673–709.
- FABRIS, G. 1984 *J. Fluid Mech.* **140**, 355–372.
- FERRÉ, J. A. & GIRALT, F. 1989 *J. Fluid Mech.* **198**, 27–64.
- GRANT, H. L. 1958 *J. Fluid Mech.* **4**, 149–190.
- KAWALL, J. G. & KEFFER, J. F. 1982 *In Turbulent Shear Flows 3* (ed. L. J. S. Bradbury, F. Durst, B. E. Launder, F. W. Schmidt & J. H. Whitelaw). Springer.
- LARUE, J. C. & LIBBY, P. A. 1974*a* *Phys. Fluids* **17**, 873–878.
- LARUE, J. C. & LIBBY, P. A. 1974*b* *Phys. Fluids* **17**, 1956–1967.
- MUMFORD, J. C. 1973 Some properties of the plane turbulent jet. PhD dissertation, University of Cambridge.
- MUMFORD, J. C. 1983 *J. Fluid Mech.* **137**, 447–456.
- THOMAS, R. M. 1973 *J. Fluid Mech.* **57**, 549–582.
- TOWNSEND, A. A. 1979. *J. Fluid Mech.* **95**, 515–537.
- WYGNANSKI, I., CHAMPAGNE, F. & MARASLI, B. 1986 *J. Fluid Mech.* **168**, 31–71.